From Change Detection to Change Analytics: Decomposing Multi-Temporal Pixel Evolution Vectors

Victoria Scherelis
Zurich University of Applied Sciences, Wädenswil, Switzerland
University of Zurich, Switzerland

Patrick Laube
Zurich University of Applied Sciences, Wädenswil, Switzerland
University of Zurich, Switzerland

Michael Doering
Zurich University of Applied Sciences, Wädenswil, Switzerland

Abstract

Change detection is a well-established process of detaining spatial and temporal changes of entities between two or more timesteps. Current advancements in digital map processing offer vast new sources of multitemporal geodata. As the temporal aspect gains complexity, the dismantling of detected changes on a pixel-based scale becomes a costly undertaking. In efforts to establish and preserve the evolution of detected changes in long time series, this paper presents a method that allows the decomposition of pixel evolution vectors into three dimensions of change, described as directed change, change variability, and change magnitude. The three dimensions of change compile to complex change analytics per individual pixels and offer a multi-faceted analysis of landscape changes on an ordinal scale. Finally, the integration of class confidence from learned uncertainty estimates illustrates the avenue to include uncertainty into the here presented change analytics, and the three dimensions of change are visualized in complex change maps.

2012 ACM Subject Classification Information systems → Spatial-temporal systems

Keywords and phrases Digital map processing, spatio-temporal modelling, land-use change

Digital Object Identifier 10.4230/LIPIcs.GIScience.2023.65

Category Short Paper

Funding Swiss National Science Foundation under Grant number 200021_188692/1.

Acknowledgements We thank Dominic Lüönd for his support with Figure 3.

1 Introduction

Change detection (CD) is the process of capturing the spatial and temporal changes of individual pixels, objects, or larger phenomena. Requiring a minimum of two timesteps, the most common types of change detection include pixel-based (PBCD) and object-based change detection (OBCD). These differ in that PBCD is focused on pixel-wise changes and usually on the spectral value of the individual pixel with no spatial relevance to its neighbors [7], and OBCD on the object represented by the pixels and grouping/segmenting the pixels into clusters of their respective categories [1]. Within the very mature field of CD, many reviews have been published to organize the different CD types [1, 7] and the vast methods and techniques used to detect changes within the various categories [2]. Current advances in CD are mostly built on existing foundations and are focused on the development of automatic change detection algorithms tailored to specific topics and based on complex neural networks or other deep learning algorithms [5].

A large application field of CD is in detecting land use and land cover (LULC) changes [4, 13], including habitat changes in riverine environments [11], the topic of the here presented study. Both PBCD and OBCD are used in LULC, mostly identifying changes between only two or three timesteps and focused on satellite data or aerial imagery [4, 13]. While some studies exist that incorporate multiple timesteps, such as in Tonolla et al. [11], there is a general lack in CD application with a large temporal depth of more than three timesteps, specifically in applying CD methods between individual timesteps of such large multitemporal data. In addition, the majority of CD methods are focused on remote sensing based data which reflect changes only since the 1940s and may already represent disrupted environments. Historical maps offer a unique perspective on pre-digital and perhaps pre-modified times, yet the application of CD methods on historical map sources is poorly represented within the literature with only few scattered examples [8]. The establishment and preservation of CD in longer time series is a costly undertaking and hence methods analytically exploiting such data are rarely seen. However, efforts in conceptualizing PBCD are well underway as space-time relationships are at the core of GIS research [3]. With rapid advancements in utilizing machine learning based digital map processing [9], more extensive sources of time series become available, offering new opportunities for exploiting such data, as shown in this study.

Visualization of the CD between two or three timesteps are shown in several studies in forms of change maps. These change maps of very few timesteps visualize changes on a binary scale of either 'change' or 'no change' [5] or show separate maps of the conditions per timestep [4, 13]. Visualization of larger temporal extent tend to show the change event of largest magnitude of a pixel [6], resulting in a rather static perspective of the observed changes. The visualization approaches of CD within the literature poorly represent the potentially very rich dynamic nature of the changes through time.

This paper presents a novel approach for the quantitative analysis of rich raster data time series, allowing an in depth analysis of detailed change evolution vectors per individual pixel. The experimental part of the paper illustrates the methods for multitemporal PBCD from Switzerland's historical maps. The pixel-wise change analytics incorporate 6 timesteps between 1876-1946. Change is decomposed into three dimensions that are visualized in three separate maps. A pixel flow chart illustrates changes between landuse classes. In addition, the change analytics also incorporate class confidence (learned uncertainty) per pixel, as model-inherent uncertainty is introduced in the extraction process from historical maps.

2 Methods

Fig. 1 illustrates the conceptual workflow from the historical map inputs to the pixel-wise change analytics. The components of the workflow are described in detail below.

Data pre-processing. The data inputs used in this study are classified pixel clusters extracted from the historical Siegfried map series of Switzerland. Based on training data, hydrological features (i.e. rivers, wetlands) are defined and grouped by certain criteria of their appearance on the maps [10] for extraction. The pixels representing these features are then extracted from the maps by deep learning algorithms [12] which output predictions in form of classified pixel clusters (Fig. 1a). A type of model-inherent uncertainty based on learned confidence estimates (LCE) are an additional output from the extraction process (see [12] for details) and the basis to determine class confidence/ uncertainty in this study. For further application in terms of habitat changes in ecohydrological environments, the predictions are reclassified based on a hierarchical classification scheme from aquatic to

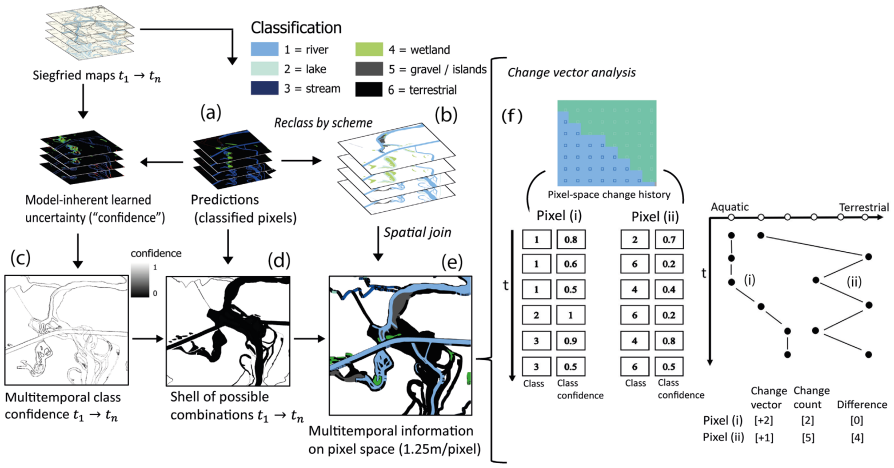

Figure 1 Conceptual workflow for multi-temporal change detection and derivation of pixel-wise change analytics ($t = time$).

terrestrial classes to determine their directed transition between the class types (Fig. 1b). The terrestrial class 6 presents any pixel unclassified from the predictions. Although the methods are presented here in the context of habitat succession, they are applicable for any geodata time series with attributes on an ordinal scale.

Integration of model-inherent uncertainty. Learned confidence estimates (LCE) show class uncertainty per pixel of the four hydrological feature classes of rivers, wetlands, lakes, and streams. Each pixel thus has 4 confidence values between 0-1 which depicts the models' uncertainty of that pixels predicted class. To integrate the LCE, the classified pixels in the predictions and the uncertainty estimates of the class identified in the associated prediction, hereafter class confidence, are extracted by a conditional evaluation. For each pixel in each timestep, the associated class confidence is then represented in the change analytics. Based on the available timesteps, the mean of the class confidence per pixel is calculated to depict the average multitemporal class confidence per pixel from $t_1 \rightarrow t_n$ (Fig. 1c). Note, LCE were available only for the first four timesteps. Thus, the represented class confidence of the time series are based on the average of the first four timesteps.

Integration of multitemporal information. For computational purposes and to avoid large amounts of terrestrial pixels, a shell of all possible multitemporal combinations was derived. The shell can be described as a sparsely populated array which occupies a pixel space when one classified pixel within any of the timesteps from $t_1 \rightarrow t_n$ occupies that pixel space, either from the predictions or from the LCE (Fig. 1d). Based on their spatial distribution, the information of the reclassified pixels were joined on to the shell. From a multitemporal perspective, not all pixel spaces have an associated class within all timesteps as the hydrological features represented by the classes change through time. Thus, pixel-spaces with no associated class in a given timestep are assigned the terrestrial class. The new dataset then holds information on the class of each pixel-space through time (Fig. 1e).

Change analytics and change vector analysis. A common CD method is the change vector analysis which can be described as the difference between the spectral pixel vector of two images [13]. The method is adapted and modified to identify the change direction and magnitude of class memberships per pixel in a multitemporal dataset with 6 timesteps (Fig. 1f). On an ordinal scale between aquatic and terrestrial, the *directed change* between two timesteps is evaluated as $DC = \sum_{n=1}^{i=1} \frac{x_{i+1} - x_i}{|x_{1+1} - x_i|}$, where DC is the change vector and x

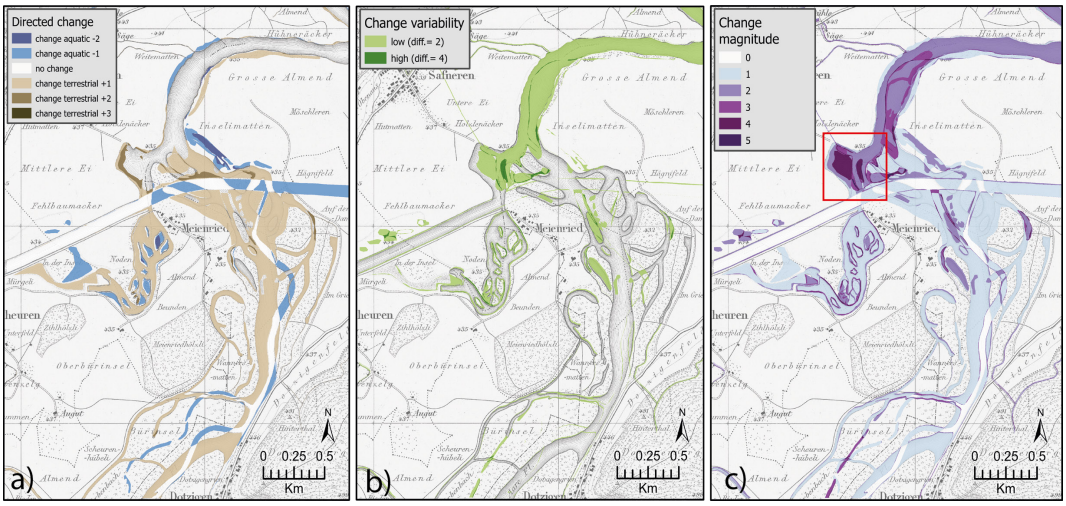

Figure 2 Visualization of the three dimensions of change in the pixel-wise change analytics, applied on a region of the Aare river in Switzerland. The background shows the 1876 Siegfried map before channelization. The red outline in (c) highlights a section for which the pixel flow paths through time are shown in Fig.3. Data source swisstopo.ch.

is a pixel of timestep i. In this equation, the difference between x_{i+1} and x_i is divided by the absolute value of that difference. This results in a value of +1 if x_{i+1} is greater than x_i (i.e., a change towards terrestrial) and -1 if x_{i+1} is less than x_i (i.e., a change towards aquatic). The expression evaluates to 0 if there is no change. The sum of the expression from $t_1 \rightarrow t_n$ then results in a change vector presenting multitemporal *directed changes*, the first dimension of the here presented change analytics.

The second dimension includes an evaluation of *change magnitude* (CM) of all changes which occurred between consecutive timesteps, described by $CM = \sum_{n=1}^{i=1} |x_{i+1} - x_i| > 0$. For each timestep i, the expression $|x_{i+1} - x_i| > 0$ evaluates to TRUE if there was a class change in x between i and $i+1$, and FALSE if otherwise. The absolute values ensure a positive expression regardless of the direction of change.

Lastly, true changes with direction are differentiated from *change variability*, where frequent changes between individual classes occur with no clear direction. This difference is evaluated by $CVar = [CM] - [|DC|]$ and depicts the third dimension of change. As exemplified in pixel (i) and (ii) in Figure 1(f), large differences between CM and $|DC|$ indicate that the class membership of the particular pixel frequently fluctuated between specific classes, whereas small to no differences indicate true directional change of the class towards aquatic or terrestrial. The change analytics per pixel can then be visualized by the calculated difference to show pixels with multitemporal variability. Where $CVar > 0$, the DC values are visualized to show the relative magnitude and direction of pixels that observed multitemporal change.

3 Results and Discussion

The detailed change analytics per individual pixel showed regions of directional change as well as regions of variability over the investigated time series of 1876 to 1946, with a timestep roughly every 14 years. The presented methods allowed the decomposition of pixel evolution vectors into three dimensions of change. Fig. 2 visualizes these dimensions of change for a

Table 1 Areas of directed change and change variability with averaged class confidence.

(1.25m/pixel)	Area (m^2) full map sheet	Average confidence
High variability	94'139	0.65
Low variability	2'700'396	0.84
Change aquatic	881'232	0.93
Change terrestrial	2'294'343	0.91

section of the map sheet under study. Fig. 2(a) depicts the dimension of directed change towards terrestrial or aquatic classes with the respective magnitude, regions where no changes occurred are shown in white. Fig. 2(b) illustrates change variability, the change dimension where pixels observed frequent alternations between specific classes (high). Some (low) change variability is observed when the classes alternate at least twice over the time series, differences of three (diff=3) or change variability higher than four variations (diff>4) where not observed. Fig. 2(c) visualizes the change magnitude observed per pixel throughout the time series, the third dimension of change.

Table 1 summarizes the areas which observed directed change and change variability, with the averaged multitemporal class confidence per pixel from the change analytics, for the map sheet TA 124 under study. The results show that the majority of pixels changed towards the terrestrial class or observed low variability, meaning that class alternations were only observed once or twice in those pixels. The class confidence was relatively low for regions that observed high variability, indicating that high variability in class changes also introduces larger uncertainties in class confidence as the class membership defined per timestep are less certain and could likely be identified as other classes in the specific timestep.

The change analytics enabled us to quantify the path of changes of each individual pixel. With six class types and 6 timesteps, over 1000 combinations of class changes were observed within the change analytics. Figure 3 illustrates the observed paths of individual pixels and their classes through time. The region of path combinations shown is outlined in red in Fig. 2c. Overall, the change history shows that terrestrial and lake classes steadily increased over time. Rivers and streams overall decreased with small increases between individual timesteps while gravel deposits and islands steadily decreased. Wetlands varied throughout the time series but generally increased over time.

4 Conclusion and Outlook

In this article, we proposed a novel approach to investigate changes in raster based data time series, generating multi-dimensional change analytics per individual pixels. The here presented methods allowed the decomposition of pixel evolution vectors into three dimensions

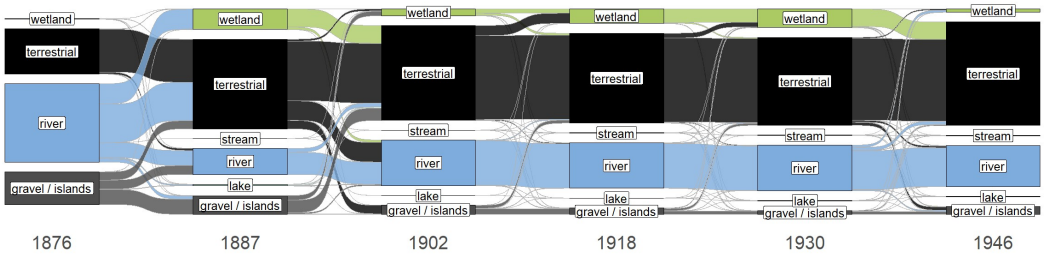

Figure 3 Flow paths of pixels and their observed classes through time (R package parcats).

of change: directed change, change variability, and change magnitude. The change analytics can be visualized by complex change maps depicting the three dimensions of change observed per pixel-space. With a unique application of PBCD on historical map sources, the change analytics included 6 timesteps and incorporated class confidence per pixel. Overall, the here presented methods offer differentiated insights in complex change dynamics, and do so considering uncertainty.

In terms of future work, we aim to incorporate the LCE for the remaining timesteps and, instead of viewing the averaged multitemporal class confidence, integrate the class confidence per class type and timestep into the pixel level change analytics. In addition, to make further use of the detail gained by the change histories, we intend to incorporate overall relative change for DC and overall absolute change for CM to capture the absolute magnitude of overall observed changes. Further timesteps and other map sheets will be investigated to test the robustness of the CD approach. In general, the change analytics described in this paper and its visualization of complex spatio-temporal data has great application potential to other fields detecting changes in multitemporal time series.

References

1 P Aplin and GM Smith. Advances in object-based image classification. *The Int. Archives of the Photogrammetry, Remote Sensing and Spatial Info. Sciences*, 37(B7):725–728, 2008.

2 Priti Attri, Smita Chaudhry, and Subrat Sharma. Remote Sensing & GIS based Approaches for LULC Change Detection – A Review. *Remote Sensing*, 2015.

3 A. Comber and M. Wulder. Considering spatiotemporal processes in big data analysis: Insights from remote sensing of land cover and land use. *Transactions in GIS*, 23(5):879–891, 2019.

4 Limin Dai, Shanlin Li, Bernard J. Lewis, Jian Wu, Dapao Yu, Wangming Zhou, Li Zhou, and Shengnan Wu. The influence of land use change on the spatial–temporal variability of habitat quality between 1990 and 2010 in Northeast China. *J. of Forestry Res.*, 30(6):2227–2236, 2019.

5 Tianqi Gao, Hao Li, Maoguo Gong, Mingyang Zhang, and Wenyuan Qiao. Superpixel-based multiobjective change detection based on self-adaptive neighborhood-based binary differential evolution. *Expert Systems with Applications*, 212:118811, 2023.

6 T. Hermosilla, M. A. Wulder, J. C. White, N. C. Coops, G. W. Hobart, and L. B. Campbell. Mass data processing of time series Landsat imagery: pixels to data products for forest monitoring. *Int. J. of Digital Earth*, 9(11):1035–1054, 2016.

7 Masroor Hussain, Dongmei Chen, Angela Cheng, Hui Wei, and David Stanley. Change detection from remotely sensed images: From pixel-based to object-based approaches. *ISPRS J. of Photogrammetry and Remote Sensing*, 80:91–106, 2013.

8 L. A. James, M. E. Hodgson, S. Ghoshal, and M. M. Latiolais. Geomorphic change detection using historic maps and DEM differencing: The temporal dimension of geospatial analysis. *Geomorphology*, 137(1):181–198, 2012.

9 Chenjing Jiao, Magnus Heitzler, and Lorenz Hurni. A survey of road feature extraction methods from raster maps. *Transactions in GIS*, 25(6):2734–2763, 2021.

10 Victoria Scherelis, Michael Doering, Marta Antonelli, and Patrick Laube. Hydromorphological Information in Historical Maps of Switzerland: From Map Feature Definition to Ecological Metric Derivation. *Annals of the Am. Asso. Geographers*, pages 1–18, 2023.

11 Diego Tonolla, Martin Geilhausen, and Michael Doering. Seven decades of hydrogeomorphological changes in a near-natural and a hydropower-regulated pre-Alpine river floodplain in Western Switzerland. *Earth Surface Proc. and Landforms*, page 5017, 2020.

12 Sidi Wu, Magnus Heitzler, and Lorenz Hurni. Leveraging uncertainty estimation and spatial pyramid pooling for extracting hydrological features from scanned historical topographic maps. *GIScience & Remote Sensing*, 59(1):200–214, 2022.

13 Song Xiaolu and Cheng Bo. Change detection using change vector analysis from landsat tm images in wuhan. *Procedia Environmental Sciences*, 11:238–244, 2011.